Volume 58(1): 1–15, 2010
Journal of Histochemistry & Cytochemistry
http://www.jhc.org

ARTICLE

Analysis of Cell Type–specific Expression of CK1ε in Various Tissues of Young Adult BALB/c Mice and in Mammary Tumors of SV40 T-Ag–transgenic Mice

Anja C. Utz, Heidrun Hirner, Annette Blatz, Andreas Hillenbrand, Bernhard Schmidt, Wolfgang Deppert, Doris Henne-Bruns, Dietmar Fischer, Dietmar R. Thal, Frank Leithäuser,[1] and Uwe Knippschild[1]

Departments of General, Visceral, and Transplantation Surgery (ACU,HH,AB,AH,BS,DH-B,UK), Experimental Neurology (DF), and Pathology (FL), and Laboratory of Neuropathology, Institute of Pathology (DRT), University of Ulm, Ulm, Germany, and Heinrich-Pette Institute for Experimental Immunology and Virology, University of Hamburg, Hamburg, Germany (WD)

SUMMARY Casein kinase 1 epsilon (CK1ε) is involved in various cellular processes, including cell growth, differentiation, and apoptosis, vesicle transport, and control of the circadian rhythm. Deregulation of CK1ε has been linked to neurodegenerative diseases and cancer. To better understand the cell type–specific functions of CK1ε, we determined its localization by immunhistochemistry in tissues of healthy, young adult BALB/c mice and in mammary tumors of SV40 T-antigen–transgenic mice. CK1ε expression was found to be highly regulated in normal tissues of endodermal, mesodermal, and ectodermal origin and in neoplastic tissue of mammary cancer. The data presented here give an overview of CK1ε reactivity in different organs under normal conditions and outline changes in its expression in mammary carcinomas. Our data suggest a cell/organ type–specific function of CK1ε and indicate that tumorigenic conversion of mammary glands in SV40 T-antigen–transgenic mice leads to downregulation of CK1ε. This manuscript contains online supplemental material at http://www.jhc.org. Please visit this article online to view these materials.

(J Histochem Cytochem 58:1–15, 2010)

KEY WORDS
CK1ε
SV40 T-Ag–transgenic mice
mammary tumors
cell type–specific expression
signal transduction
immunohistochemistry

CASEIN KINASE 1 EPSILON (CK1ε) belongs to the CK1 gene family of ubiquitously expressed second-messenger independent monomeric serine/threonine–specific kinases. In mammals, seven CK1 isoforms, namely CK1α, -β, -γ_{1-3}, -δ, and -ε, and their various splice variants have been described. They all contain a highly conserved kinase domain, a short N-terminal domain of 6 to 76 amino acids, and a highly variable C-terminal domain of 24 to more than 200 amino acids (reviewed in Gross and Anderson 1998; Knippschild et al. 2005). The constitutive phosphotransferase activity of CK1 isoforms is tightly controlled by several mechanisms. For example, the closely related isoforms CK1δ and -ε, which share a 98% identity at the amino acid level in their catalytic domain, are regulated by autophosphorylation, dephosphorylation, and proteolytic cleavage. Members of the CK1 family are found in the nucleus, the cytoplasm, and in the plasma membrane (reviewed in Gross and Anderson 1998; Knippschild et al. 2005). By phosphorylating many different substrates bearing either a canonical or non-canonical consensus sequence (Gross and Anderson 1998; Marin et al. 2003; Okamura et al. 2004b; Bustos et al. 2005), they modulate the activity of key regulator proteins involved in many cellular processes, such as cell differentiation (Peters et al. 1999; Amit et al. 2002; Liu et al. 2002; Davidson et al. 2005; Zeng et al. 2005; Swiatek et al. 2006), cell proliferation, apoptosis (Beyaert et al. 1995; Desagher

Correspondence to: Uwe Knippschild, Department of General, Visceral, and Transplantation Surgery, University of Ulm, Steinhövelstr. 9, 89075, Ulm, Germany. E-mail: uwe.knippschild@uniklinik-ulm.de
[1]These authors shared senior authorship.
Received for publication July 9, 2009; accepted August 7, 2009 [DOI: 10.1369/jhc.2009.954628].

et al. 2001; Izeradjene et al. 2004; Takenaka et al. 2004; Zhao et al. 2004), circadian rhythm (Camacho et al. 2001), chromosome segregation (Brockman et al. 1992; Behrend et al. 2000a,b; Petronczki et al. 2006), and vesicle transport (Brockman et al. 1992; Milne et al. 2001; Behrend et al. 2000b). Because CK1 is involved in so many different cellular processes, mutations and/or changes in the activity of CK1 isoforms have a great impact on the development of several diseases, including neurodegenerative diseases (Kuret et al. 1997; Walter et al. 1998; Schwab et al. 2000; Yasojima et al. 2000; Ebisawa et al. 2001; Toh et al. 2001; Takano et al. 2004; Xu et al. 2005) and cancer (Elias et al. 1981; Maritzen et al. 2003; Bagheri-Yarmand et al. 2004; Fuja et al. 2004; Knippschild et al. 2005; Stoter et al. 2005; Brockschmidt et al. 2008). Mutations and alterations in the expression and/or activity of CK1ε have been detected in various tumor entities, e.g., in adenocarcinomas of the pancreas (Brockschmidt et al. 2008), in mammary tumors (Fuja et al. 2004), and in adenoid cystic carcinomas (Frierson et al. 2002). It is obvious that knowledge of the CK1ε expression pattern would be helpful to understanding the function of this protein.

In the present study, we examined the distribution of CK1ε in various tissues and organs of young adult, healthy BALB/c mice by immunohistochemistry (IHC) and Western blot analyses. In addition, we used real-time PCR and IHC of mammary tumors in SV40 T-Ag–transgenic mice to determine how neoplastic transformation affects CK1ε expression. Our immunohistochemical data describing the cell type– and organ-specific expression of CK1ε in BALB/c mice can be used as an anatomical basis for understanding its physiological functions. Furthermore, our data point to the possibility that downregulation of CK1ε may potentially be involved in tumorigenesis of the mammary gland.

Materials and Methods

Animals and Tissue Processing

Animal studies were performed in accordance with the guidelines of the authority of animal use and were approved by the local authorities (Regierungspräsidium Tübingen). BALB/c mice and SV40 T-Ag–transgenic mice, strain WAP-T-NP8 (Schulze-Garg et al. 2000) (henceforward called WAP-T mice), were bred in the Animal Research Center of the University of Ulm. WAP-T mice are a well-established animal model for mammary cancer, allowing us to study morphological and biological qualities of different intraductal and invasive carcinomas. In these mice, an epitope-tagged T-Ag controlled by the WAP promoter, is induced in lactating mammary epithelium by mating. On average, 5.5 months after induction, female WAP-T mice have developed mammary tumors that typically display a poorly differentiated or even anaplastic morphology.

Tissue samples from 4- to 6-week-old BALB/c male and female mice (5/5) and normal mammary glands and mammary tumors of 18 induced female WAP-T mice were immediately excised after sacrifice, and shock frozen or fixed by immersion in either 1% acetic acid in formalin, or 10% buffered neutral formalin. Bone tissue was decalcified with EDTA for several days at 4C. Fixed tissues were then dehydrated in a graded ethanol series, cleared in methyl benzoate, and embedded in paraffin. Paraffin-embedded sections were cut at 3 μm and mounted on glass slides. Frozen tissue was embedded in Tissue-Tek (Sakura; Heppenheim, Germany). Sections (5–8 μm) were cut on a cryostat microtome (Leica; Bensheim, Germany), mounted on dry glass slides, and fixed in 100% acetone for 10 min at 4C.

Primary Antibodies

The following primary antibodies were used: CK1ε-specific polyclonal rabbit antisera 712 (Brockschmidt et al. 2008) and sc25423 (H60) (Santa Cruz Biotechnology; Santa Cruz, CA), mouse monoclonal CK1ε-specific antibody 610445 (BD Biosciences; San Jose, CA), T-Ag–specific polyclonal rabbit antiserum R15 (Deppert and Pates 1979), and mouse monoclonal anti-β-actin specific antibody A5316 (Sigma-Aldrich; Hamburg, Germany).

Immunohistochemistry

Staining of Paraffin Sections. Staining procedures included deparaffinization in xylene, followed by rehydration via transfer through graded alcohols. To inhibit endogenous enzyme activity, peroxidase blocking reagent (DAKO; Glostrup, Denmark) was used. The sections were treated with the antigen retrieval solution Citra Plus, pH 6.03 (BioGenex; San Ramon, CA) in a microwave oven according to the manufacturer's instructions. Sections were then incubated with one of the CK1ε-specific antibodies (712, 1:1200; or SC25423 (H60) 1:150) at 4C overnight. After washing in Tris-HCl buffer, horseradish peroxidase–containing polymer-conjugated anti-rabbit IgG antibody (N-Histofine; Nichirei Corporation, Tokyo, Japan) was applied at room temperature for 30 min. The enzymatic reaction was developed in a freshly prepared solution of 3,3′-diaminobenzidine using DAKO Liquid DAB Substrate-Chromogen solution as a chromogen for horseradish peroxidase. The sections were then counterstained with hematoxylin and permanently mounted in Entellan (Merck; Darmstadt, Germany). Positive and negative controls were included for each case. As a negative control, the primary antiserum was omitted, with Tris-HCl buffer as a substitute. Immunohistochemical detection of T-Ag was performed as described earlier using T-Ag–specific polyclonal rabbit antiserum R15 (Schulze-Garg et al. 2000).

Staining of Frozen Sections. Frozen sections were quickly rehydrated in Tris-HCl buffer. Endogenous enzyme activity was blocked as described above. Sections were then incubated with CK1ε-specific polyclonal serum 712 (1:1000) for 40 min at room temperature. Slides were washed in Tris-HCl buffer, and the DAB reaction was performed as described above. Next, sections were counterstained with hematoxylin.

Grading System. Sections were graded according to the intensity of the CK1ε-specific staining. Intensity levels of the CK1ε-specific staining were graded as: −, negative; +, weak; ++, moderate; or +++, strong. A slash indicates simultaneous expression of different intensities, e.g., $^{-/++}$ indicates negative and moderately positive staining in one cell type or microanatomical region.

Western Blot Analysis. For the detection of CK1ε and β-actin protein, murine tissues were lysed in NP40 lysis buffer. Extracts were clarified by centrifugation, and the protein concentration of the lysates was determined. Seventy-five μg of the protein extract was separated on 12.5% SDS-polyacrylamide gels and transferred onto a nitrocellulose blotting membrane (Hybond C super; GE Healthcare, Chalfont St. Giles, UK). The membranes were probed with either CK1ε-specific monoclonal antibody 610445 (BD Biosciences) or with the β-actin-specific antibody (Sigma, Germany). Immunocomplexes were detected using anti-mouse or anti-rabbit peroxidase-conjugated IgG, followed by chemiluminescence detection (ECL; GE Healthcare).

Gene Expression Analysis. Total RNA was isolated from normal mammary glands and breast tumors of induced WAP-T mice using the RNeasy Kit (Qiagen; Hilden, Germany). Total RNA (1.5 μg) was reverse transcribed into cDNA using the RT^2 First Strand Kit (SuperArray Bioscience Corp.; Frederick, MD). Profiling of CK1ε expression levels was done as described by the manufacturer (SuperArray Bioscience Corp.). The reactions were carried out in an Applied Biosystems 7500 Fast Real-Time PCR System (Foster City, CA). The results were read out with the 7500 Fast System SDS Software.

Results

CK1ε Expression Levels in Young Adult Mice

To characterize the CK1ε expression levels in various tissues and organs of BALB/c mice, equal amounts of the different protein extracts were analyzed by Western blotting. Although CK1ε is widely expressed, expression levels varied significantly among tissues (Figure 1). CK1ε was markedly expressed in the lung and brain; intermediate expression levels of CK1ε were found in the heart, ovary, muscle, liver, uterus, and testis; and low expression levels could be observed in the thymus, mammary gland, eye, colon, pancreas, bladder, and kidney. An increased amount of a faster migrating form of CK1ε was seen in the spleen (Figure 1).

Comparison of the Immunoreactivity of Two CK1ε-specific Antibodies in Paraffin-embedded Tissues

To analyze the cell type–specific expression of CK1ε in histological sections of different tissues and organs, immunohistology was carried out with either CK1ε-specific polyclonal rabbit antiserum 712 (Brockschmidt et al. 2008) or rabbit polyclonal CK1ε-specific antibody sc25423 (Santa Cruz Biotechnology). Comparative analysis revealed a similar reactivity of both antibodies in all paraffin-embedded tissues, as illustrated by immunohistochemical staining of the bladder and prostate (see supplementary Figure SF1).

Detection of CK1ε in Frozen and Paraffin-embedded Tissues

CK1ε-specific antiserum 712 detected CK1ε in both frozen and paraffin-embedded tissues, with similar staining strength and specificity for the heart, lung,

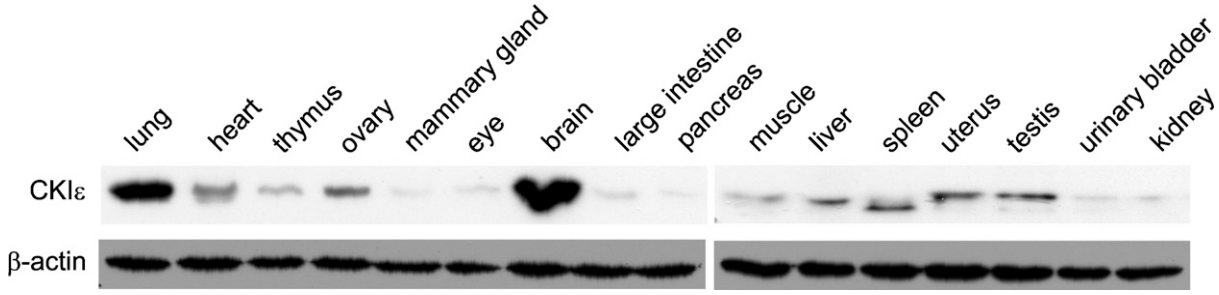

Figure 1 Expression level of CK1ε in different tissues and organs of 4–6-week-old BALB/c mice. Specimens were homogenized, and equal protein amounts (75 μg) were separated by SDS-PAGE. CK1ε protein levels were detected by Western blotting using a CK1ε-specific monoclonal antibody (BD Biosciences). Equal loading of extracted proteins was determined by probing a second membrane with a β-actin–specific monoclonal antibody.

Table 1 Localization and levels of CK1ε in 4- to 6-week-old BALB/c mice

Thymus	
Cortex thymocytes	−/+
Medulla thymocytes	−/+
Medulla stroma cells	++/+++
Bone marrow	
Hematopoietic stem cells	−/+/++
Megakaryocytes	++/+++
Lymph node/MALT	
Germinal center	++
Mantle zone	−
Primary follicle	−
T zone	+
Spleen	
Red pulp	++
White pulp	−/+
Sinusoidal lining cells	+++
Megakaryocytes	+++
Muscle cells	
Skeletal	−/++
Cardiac	−/++
Smooth	++
Vascular endothelium	
Arteries	++
Veins	+
Lymphatics	+
High endothelial venoles	++
Mesothelial cells	+
Connective tissue	
Adipocytes (univacuolar)	+/++
Adipocytes (polyvacuolar)	++
Fibroblasts/fibrocytes	−/+
Chondrocytes	−
Osteoblasts	+++
Osteocytes	+
Alimentary tract	
Esophageal squamous epithelium (basal cell layer)	++
Esophageal squamous epithelium (stratum granulosum)	+++
Stomach, chief cells	+++
Stomach, parietal cells	+/++
Stomach, mucous neck cells	+
Surface epithelium	++
Intestine, absorptive cells	+++
Intestine, goblet cells	−/++
Intestine, paneth cells	−/+
Salivary glands	
Serous epithelial cells	−
Mucous epithelial cells	+
Myoepithelium	−
Ductal epithelium	++
Pancreas	
Exocrine gland, acinar cells	−/+
Exocrine gland, duct epithelium	+
Islets	++/+++
Liver	
Hepatocytes	++
Intrahepatic bile ducts	++
Adrenal	
Stratum granulosum	++
Stratum fasciculatum	+
X zone	+++
Medulla	−/+++

Table 1 (*Continued*)

Hypophysis	
Adenohypophysis	+++
Neurohypophysis	+++
Pars intermedia	+++
Thyroid gland	
Follicular epithelium	+/++
Eye	
Sclera	−
Cornea	−
Iris stroma	++
Iris posterior epithelial lining	+
Ciliary muscle	+
Ciliary epithelium	++
Lens capsule	−
Cuboidal epithelium of the lens	+
Lens fibers	
Cortex	++
Nucleus	−
Retina	
Choroid	++
Retinal pigment epithelium	+
Photoreceptors outer segment	−
Photoreceptors inner segment	+++
Outer nuclear layer	−
Outer plexiform layer	++
Inner nuclear layer	−
Inner plexiform layer	+
Ganglion cell layer	+
Respiratory tract	
Upper aerodigestive tract, squamous epithelium, basal cell layer	+++
Upper aerodigestive tract, squamous epithelium, superficial cell layer	+++
Respiratory epithelium	+++
Type 1 pneumocytes	+
Type 2 pneumocytes	++
Pleura	+
Nervous system	
Peripheral nervous system	
Trigeminal ganglion	
Nerve cell perikaryon	+++
Peripheral nerve fiber	(+)
Spinal ganglion	
Nerve cell perikaryon	+++
Peripheral nerve fiber	(+)
Central nervous system	
Spinal cord	
Gray matter, nerve cell perikaryon	+++
Gray matter neuropil	+
White matter/astrocytes	−/+
Brain	
Nerve cell perikaryon/neuropil	
Cerebral neocortex	++/(+)
Hippocampus	++/(+)
Basal ganglia	++/(+)
Hypothalamus	++/(+)
Thalamus	++/(+)
Midbrain	+ − ++/(+)
Pons	+ − ++/(+)
Medulla oblongata	+ − ++/(+)
Purkinje cells/cerebellum	−
Granule cells/cerebellum	−

Table 1 (*Continued*)

Nervous system	
Brain	
Dentate nucleus	−
White matter/astroglia	−/++
Urinary tract	
Glomerulum	−/+
Tubulus epithelium	++/+++
Collecting duct epithelium	+
Urothelium, basal cells	+
Urothelium, umbrella cells	++
Female genital tract	
Oocytes	+/++
Immature ovarian follicle, follicular epithelium	++
Mature ovarian follicle, follicular epithelium	−/+
Theka cells	+
Fallopian tube	++
Uterus endometrium	++/+++
Uterus stroma cells	+
Vaginal epithelium	+++
Male genital tract	
Germinal cells, spermatogonia	+++
Spermatocytes	++
Sertoli cells	+
Leydig cells	++
Epididymis epithelium	+++
Deferent duct epithelium	+++
Prostate gland	++/+++
Seminal vesicle	++
Skin and skin appendages	
Epidermis (basal layer)	++
Epidermis (stratum granulosum)	+++
Sebacous gland	+
Hair follicle epithelium	++
Haderian gland	+
Mammary gland, glandular epithelium	++
Mammary gland, myoepithelium	−

Intensity levels of the CK1ε-specific staining were graded as: −, negative; +, weak; ++, moderate; or +++, strong. Slash indicates simultaneous expression of different intensities, e.g., −/++ indicates negative and moderately positive staining in one cell type. Staining results were nearly identical independent of the CK1ε-specific antibody [712 and (H60) sc-25423] having been used. MALT, mucosa-associated lymphoid tissue.

liver, and colon (see supplementary Figure SF2). However, the quality in regard to the morphology of the frozen sections was quite variable, whereas the paraffin sections exhibited reliable and consistent results of good quality. In areas of dense staining, individual cells could still be identified in paraffin sections, but not in frozen sections, as shown in supplementary Figure SF2.

Detection of CK1ε Immunoreactivity in Paraffin-embedded Tissues of Young Adult BALB/c Mice

CK1ε reactivity in various paraffin-embedded tissues of 10 young adult BALB/c mice (5 males/5 females) determined by IHC is summarized in Table 1. These results correspond well with our results obtained by Western blot analysis.

Subcellular Antigen Distribution

In most immunoreactive cells, CK1ε was localized to the cytoplasm. Only some cell populations, e.g., male germ cells, displayed a nuclear immunoreactivity (Figure 2S).

Alimentary Tract

In the keratinized squamous epithelium lining, the esophagus, and parts of the murine stomach, CK1ε was moderately positive in the basal, parabasal, and intermediate cell layers, increasing to strong staining levels in the superficial stratum (Figure 2A). The various cell types that constitute the epithelium of the glandular part of the murine stomach showed a heterogeneous CK1ε expression pattern. At the base of the crypts, chief cells were strongly CK1ε positive, in contrast to parietal cells, which expressed only low to intermediate amounts of CK1ε. Toward the more superficial parts of the gastric mucosa, mucous neck cells and surface epithelial cells were weakly CK1ε positive (Figures 2B1, 2B2). Intense CK1ε positivity was observed in the absorptive epithelium of the small and large intestine (Figure 2C). Some goblet cells expressed moderate levels of CK1ε, whereas a subset of goblet cells lacked CK1ε (Figures 2C and 2D). In the small intestine, Paneth cells were CK1ε negative or weakly positive (Figure 2C).

Large Exocrine Glands of the Alimentary Tract

The large salivary glands draining in the oral cavity were composed of CK1ε-negative serous and myoepithelial cells and mucous cells that were weakly positive for CK1ε. The duct epithelia displayed a moderate CK1ε staining intensity (Figure 2E). In the serous glandular epithelium of the exocrine part of the pancreas, CK1ε expression was low and in some cells negative. The cuboidal/columnar epithelium lining the pancreatic ducts showed weak CK1ε expression (Figure 2F and inset). In the liver, moderate CK1ε staining was seen in the hepatocytes (Figure 2G). Staining of the parenchyma was diffuse throughout the different zones of the liver acinus. The intrahepatic bile ducts demonstrated intermediate CK1ε immunoreactivity (Figure 2G inset).

Endocrine Organs

We confined our immunohistochemical analysis of the endocrine organs to the pancreas (Figure 2F), the adrenal (Figure 2H), the thyroid (Figure 2I), and the anterior lobe of the hypophysis (Figures 3A and 3B). Other components of the endocrine system, i.e., the parathyroid gland and the diffuse endocrine system of the mucosal surfaces, were excluded from our studies, owing to difficulties in anatomical preparation or in histological detection, respectively.

The Journal of Histochemistry & Cytochemistry

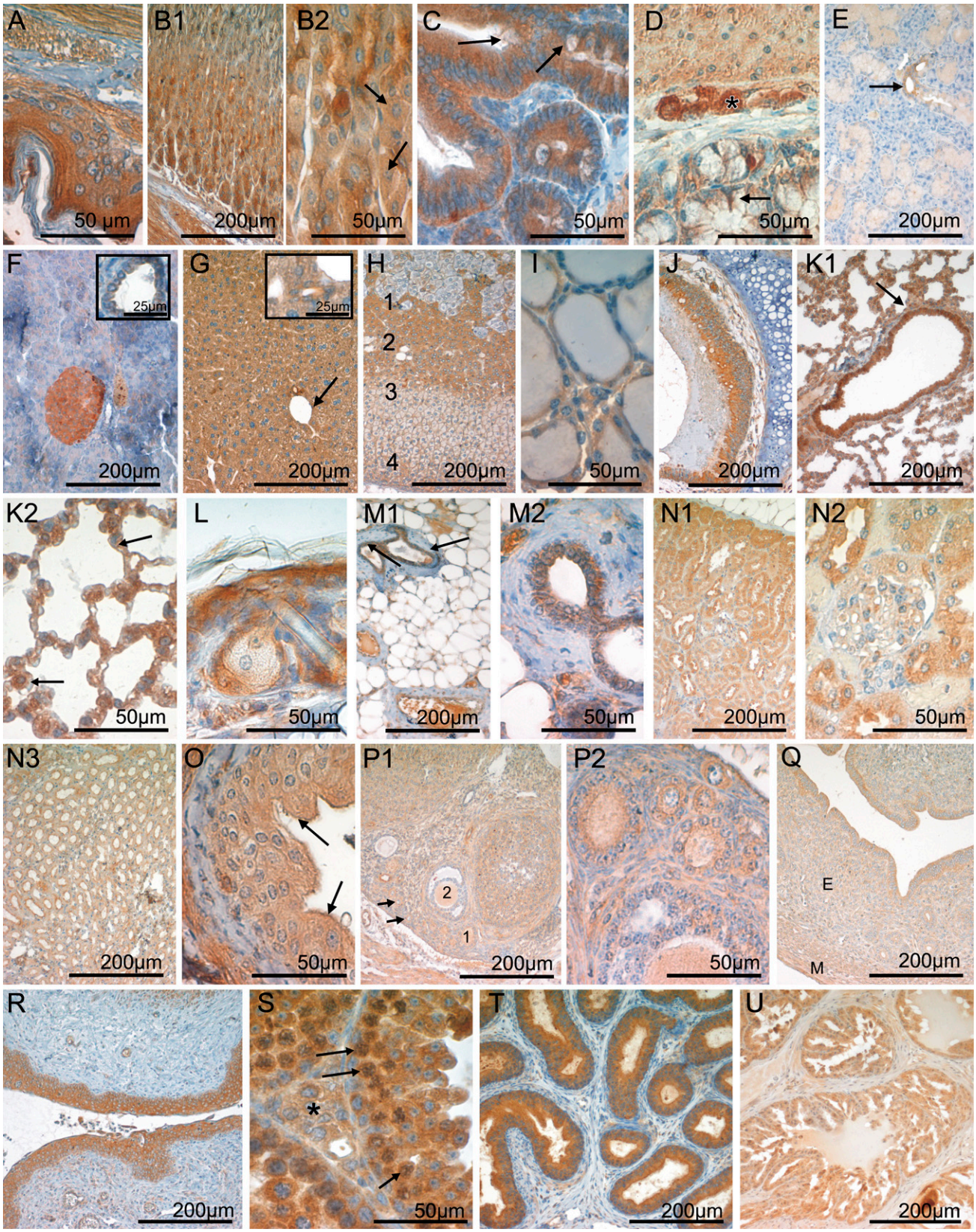

Cells of the endocrine pancreas, i.e., the Islets of Langerhans, were moderately to strongly CK1ε positive (Figure 2F). Without resorting to double immunostaining techniques, it was not possible to further specify CK1ε expression in different Langerhans cell subsets, as defined by the peptide hormone produced. In young adult mice, the adrenal cortex consisted of the moderately CK1ε-positive zona glomerulosa, the weakly stained zona fasciculata, and the strongly CK1ε-expressing X zone (Figure 2H). CK1ε expression was markedly heterogenous in the adrenal medulla, which contained strongly CK1ε-positive cells as well as a CK1ε-negative subset (Figure 2H). The thyroid gland showed low to intermediate levels of CK1ε expression in the follicular epithelium (Figure 2I).

All three parts of the pituitary gland exhibited cytoplasmic CK1ε expression. There was no obvious variation in expression among the different cell types of the adenohypophysis (Figures 3A and 3B). In the neurohypophysis, pituicytes showed strong cytoplasmic CK1ε immunoreactivity (Figure 3C). The neuropil was moderately labeled.

Respiratory Tract

The ciliated respiratory epithelium lining the trachea (Figure 2J) and the proximal branches of the bronchial tree (Figure 2K1) was intensely CK1ε positive. CK1ε expression was reduced to weak levels upon transition to the type I pneumocytes of the respiratory bronchioles and the lung alveoli, whereas surfactant-producing type II pneumocytes retained moderate CK1ε levels (Figures 2K1 and 2K2). The small glands of the respiratory tract contained CK1ε-negative serous epithelial cells and mucous cells that displayed low amounts of CK1ε.

Skin and Skin Appendages

The squamous epithelium of the skin was moderately CK1ε positive in the basal cell layers, increasing to strong antigen expression toward the superficial parts of the epidermis. Hair follicles displayed intermediate levels of CK1ε expression. Sebaceous glands and Haderian glands were weakly CK1ε positive (Figure 2L). In the non-lactating mammary gland, moderate CK1ε expression was seen in the secretory epithelium, whereas the myoepithelium was CK1ε negative (Figures 2M1 and 2M2).

Urinary Tract

Cells of the renal glomerulum were CK1ε negative or weakly positive (Figure 2N2). This low staining intensity, in conjunction with the morphology obtainable in CK1ε immunohistochemical preparations, did not permit a more detailed assignment of CK1ε expression to specific glomerular cell populations. The tubular epithelium was strongly CK1ε positive in the intermediate part, and moderately positive in the proximal and distal sections, whereas low CK1ε expression was found in the epithelium of the collecting ducts (Figures 2N1, 2N2, and 2N3). The transitional epithelium of the ureter and the urinary bladder was weakly CK1ε positive, increasing to moderate levels in the superficial (umbrella) cells (Figure 2O).

Female Genital System

Immunohistochemical staining of the ovary revealed weak to intermediate CK1ε expression in the oocytes (Figures 2P1 and 2P2). The follicular epithelium was moderately CK1ε positive at immature stages, dropping to no or only weak staining in more-mature follicles (Figures 2P1 and 2P2). Theka cells surrounding the ovarial follicles were weakly CK1ε positive (Figures 2P1 and 2P2). The epithelia of the oviducts and the uterine mucosa displayed intermediate to strong levels of CK1ε expression, whereas the endometrial stroma cells were only weakly CK1ε positive (Figure 2Q). The squamous epithelium of the vagina was strongly CK1ε positive (Figure 2R).

Male Genital System

In the germinal epithelium of the testis, CK1ε expression was intense in the spermatogonia and slightly decreased in the course of maturation toward spermatocytes (Figure 2S). Sertoli cells were weakly CK1ε positive, and Leydig cells of the interstitium were moderately CK1ε

Figure 2 CK1ε expression in the gastrointestinal tract, endocrine glands, lung, mammary gland, skin, and urogenital tract. Fixative: acid formalin, fixation by immersion. Peroxidase reaction, dye: DAB. CK1ε-specific serum 712 was used for immunohistochemical staining of the following organs: esophagus (**A**), stomach (**B1,B2**), small intestine (**C**), colon (**D**), salivary gland (**E**), pancreas (**F**), liver (**G**), adrenal gland (**H**), thyroid gland (**I**), trachea (**J**), lung (**K1,K2**), skin (**L**), mammary gland (**M1,M2**), kidney (**N1,N2,N3**), ureter (**O**), ovary (**P1,P2**), uterus (**Q**), vagina (**R**), testis (**S**), epididymis (**T**), and prostate (**U**). In **B2**, arrows point to parietal cells. In **C** and **D**, arrows point to goblet cells. In **E**, arrow indicates the CK1ε-positive ductal epithelium. In the inset of **F**, a pancreatic duct is shown. In the liver (**G**) the arrow points to a central vein. An intrahepatic bile duct is shown in the inset of **G**. In **H**, the numbers indicate the medulla (1), the x zone (2), the zona fasciculata (3), and the zona glomerulosa (4). In **K1**, arrow indicates the bronchial epithelium. In **K2**, arrows point to type II pneumocytes. Arrows in **M1** indicate the ductal epithelium of the mammary gland. **N1** shows the renal cortex, **N2** a glomerulum, and **N3** the renal medulla. Arrows in **O** point to umbrella cells of the urothelium. In **P1**, the numbers indicate the moderate CK1ε-positive epithelium of a primary follicle (1) and a secondary follicle (2). The small primordial follicles are marked by arrows. **P2** shows several ovarian follicles of different maturation stages at high magnification. In **Q**, smooth-muscle cells of the myometrium (M) and the epithelium of the endometrium (E) are CK1ε positive. In **S**, asterisk indicates a group of Leydig cells, and arrows indicate spermatogonia. Calibration bars in all figures are as indicated.

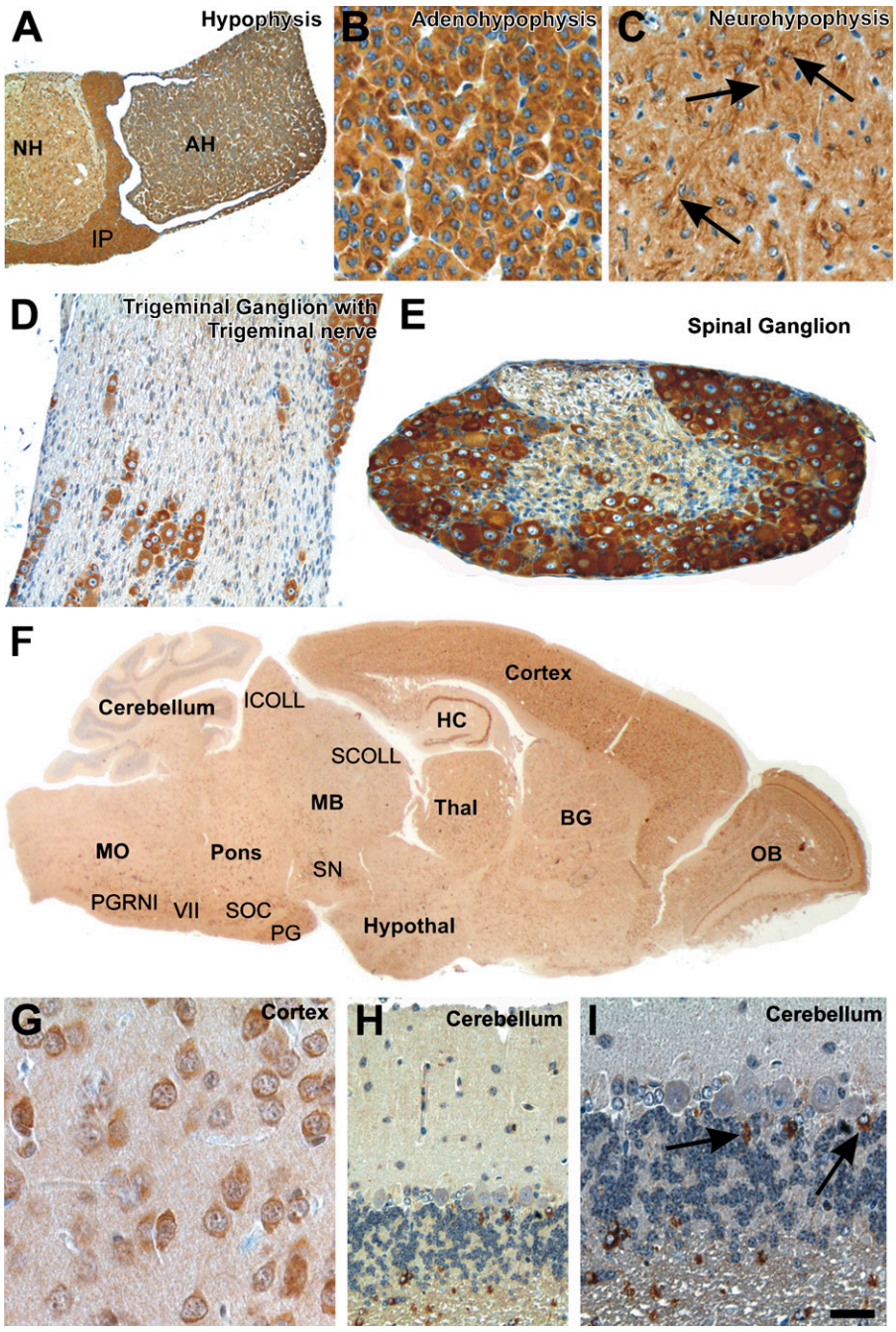

Figure 3 CK1ε expression in the nervous system. Fixative: acid formalin, fixation by immersion. Peroxidase reaction, dye: DAB. CK1ε expression in the hypophysis, the peripheral nervous system, and the central nervous system. (**A**) Cross-section of the hypophysis shows a strong CK1ε expression in the adenohypophysis (AH), neurohypophysis (NH), as well as in the intermediate part (IP). (**B**) Higher magnification of the adenohypophysis exhibits epithelial cells showing a strong cytoplasmic staining with anti-CK1ε. (**C**) Pituicytes in the neurohypophysis (arrows) show a strong coloration of the cytoplasm, including their processes. The neuropil is moderately stained. (**D,E**) Nerve cells in the ganglion trigeminale (**D**) and the spinal ganglion (**E**) are strongly labeled with anti-CK1ε in the cytoplasm. Schwann cells are only weakly marked. An axonal staining was not observed. (**F**) Saggital section of a mouse brain stained with anti-CK1ε. Nerve cells in all cortical layers are significantly stained, as well as neurons of the hippocampus (HC), olfactory bulb (OB), basal ganglia (BG), hypothalamus (Hypothal), and thalamus (Thal). In the midbrain (MB), pons, and medulla oblongata, neurons of specific nuclei express CK1ε [e.g., substantia nigra (SN), pontine gray (PG), superior olivary complex (SOC), nucleus of the facial nerve (VII), and paragigantocellular nucleus, lateral part (PGRNl)], as well as neurons of the superior (SCOLL) and inferior collicles (ICOLL). (**G**) Neurons express CK1ε in their cytoplasm, as shown, for example, in the parietal cortex. (**H,I**) Granule cells and Purkinje cells of the cerebellum do not exhibit CK1ε in detectable amounts. Here, astrocytes, including Bergmann glial cells, express CK1ε in their cytoplasm. Calibration bar in **I** is valid for **A** = 150 μm; **B,G** = 20 μm; **C,I** = 25 μm; **D,E,H** = 50 μm; **F** = 650 μm.

positive (Figure 2S). Strong CK1ε expression was observed in the epithelial lining of the epididymis and the spermatic duct (Figure 2T). The epithelial cells of the seminal vesicle and the prostate gland were strongly to moderately CK1ε positive (Figure 2U).

Immobile Cells of Mesenchymal Origin

Skeletal and cardiac muscle cells showed a heterogeneous staining pattern consisting of CK1ε-negative and CK1ε–moderately positive myocytes (Figures 4A1, 4A2, and 4B). The staining in these cell populations was mostly diffuse; however, in the myocardium, an increased staining intensity was observed in the intercalated discs. Smooth-muscle cells at the various locations showed an intermediate level of CK1ε expression (Figure 4C). The vascular endothelium of arterial vessels and high endothelial venoles (as seen in secondary lymphatic organs) (Figures 4D1 and 4D2) contained intermediate amounts of CK1ε, whereas veins and lymphatics harbored a weakly CK1ε-stained endothe-

lium (Figure 4D1). Mesothelial cells lining the peritoneal and the pleural cavity as well as the pericardium were invariably CK1ε weakly positive (Figure 4E).

Adipocytes of the plurivacuolated ("brown") and univacuolated ("white") type were weakly to moderately CK1ε positive (Figures 4F1 and 4F2). Fibrocytes, chondrocytes, and osteocytes showed no or only weak CK1ε expression (Figures 4G, 4H, and 4I). In contrast, osteoblasts were intensely CK1ε positive (Figures 4H and 4I).

Hematopoietic Cells and Immune System

Immature hematopoietic cells in the bone marrow (Figure 4J) and at sites of extramedullary hematopoiesis [i.e., the spleen (Figure 4K)] displayed varying levels of CK1ε expression, ranging from negative to strongly positive. Although strongly CK1ε-expressing megakaryocytes were readily identified by their size and distinctive morphology, it was not possible to distinguish precisely the different cell types in the bulk of hematopoietic cells on the basis of single immunostainings carried out in the present study.

In the thymus, a large population of small lymphoid cells probably representing thymocytes was CK1ε negative to weakly positive (Figure 4L). In the thymic medulla, a moderately to strongly CK1ε-positive stroma cell population was observed (Figure 4L). Lymphocytes of the secondary lymphatic organs displayed varying amounts of CK1ε expression, depending on the organ type and the microanatomical compartment. CK1ε expression tended to be strongest in the germinal centers of secondary lymphoid follicles seen in lymph nodes, whereas mantle zones and primary follicles were CK1ε negative (Figures 4M and 4N). In T zones, weak CK1ε expression was observed (Figures 4M, 4N, and 4O). In the white pulp of the spleen, no or only weak CK1ε expression was observed, corresponding to a predominating population of resting B and T lymphocytes (Figure 4K). At the border between the T/B zone and the marginal zone, macrophages, here called sinusoidal lining cells, were conspicuous by their strong CK1ε positivity. In the red pulp, the majority of cells showed intermediate CK1ε staining.

Eye

The microanatomical complexity of the retina was mirrored by a differential CK1ε expression in its various layers. The ganglion cell layer was weakly CK1ε positive (Figures 4P and 4Q). Fluorescent double staining revealed a colocalization of CK1ε staining with βIII-positive retinal ganglion cells (Figures 4R–4T). No CK1ε staining was observed in the inner nuclear layer, whereas the outer plexiform layer displayed a significant CK1ε staining intensity. The outer nuclear layer and the outer segment of the photoreceptors lacked CK1ε expression. In contrast, the inner segment of photoreceptors was CK1ε positive. CK1ε was weakly expressed by the retinal pigment epithelium (Figure 4P). Adjacent to the retina, the vascularized connective tissue of the choroidea was moderately CK1ε positive (data not shown). No CK1ε staining was seen in the sclera or the cornea (data not shown). The capsule of the lens was CK1ε negative, and the underlying cuboidal epithelium stained weakly. The fibers in the center of the lens lacked CK1ε, whereas intermediate expression levels were detected in the cortical fibers. The stroma of the iris was moderately CK1ε positive. The epithelial cells lining the posterior surface of the iris displayed weak CK1ε staining. In contrast, the epithelium covering the ciliary body was moderately CK1ε positive, whereas weak antigen expression was found in the smooth ciliary muscle (Figure 4P).

Peripheral and Central Nervous System

Peripheral Nervous System. The peripheral nerve fibers were only weakly labeled for CK1ε. Primarily the Schwann cells exhibited a slight intracytoplasmatic immunoreactivity, whereas the axons did not appear to be marked (Figure 3D). In the peripheral ganglia, the nerve cells showed a strong immunoreaction with anti-CK1ε in the soma (Figures 2D and 3D).

Central Nervous System. The cross-section of the hypophsis shows strong CK1ε expression in the adenohypophysis, the neurohypophysis, and in the intermediate part (Figures 3A–3C). CK1ε was expressed in all neurons of the olfactory bulb, cerebral cortex, and hippocampus (Figures 3F and 3G). Most neurons in the basal ganglia, hypothalamus, thalamus, midbrain, pons, and medulla oblongata also exhibited cytoplasmic staining for CK1ε (Figure 3F). Only the Purkinje and granule cells in the cerebellum did not show significant amounts of CK1ε labeling (Figures 3H and 3I). However, a subset of astrocytes was strongly marked with anti-CK1ε (Figure 3I). The neurons of the spinal cord exhibited a moderate cytoplasmatic expression of CK1ε.

CK1ε Expression Is Altered in Ductal Carcinoma of the Mammary Gland in SV40-transgenic Mice

To get hints for a role of CK1ε in tumorigenesis of mammary cancer, we used an SV40 T-Ag–inducible transgene animal model for ductal carcinoma. In this model, the tumors mostly display a poorly differentiated or even anaplastic morphology (see Figure 5; Table 2). Immunostaining revealed that expression of nuclear T-Ag in mammary epithelium preceded the development of morphologically detectable tumors. Of note, T-Ag expression was associated with a high mitotic rate. In overt neoplasia, i.e., intraductal and

The Journal of Histochemistry & Cytochemistry

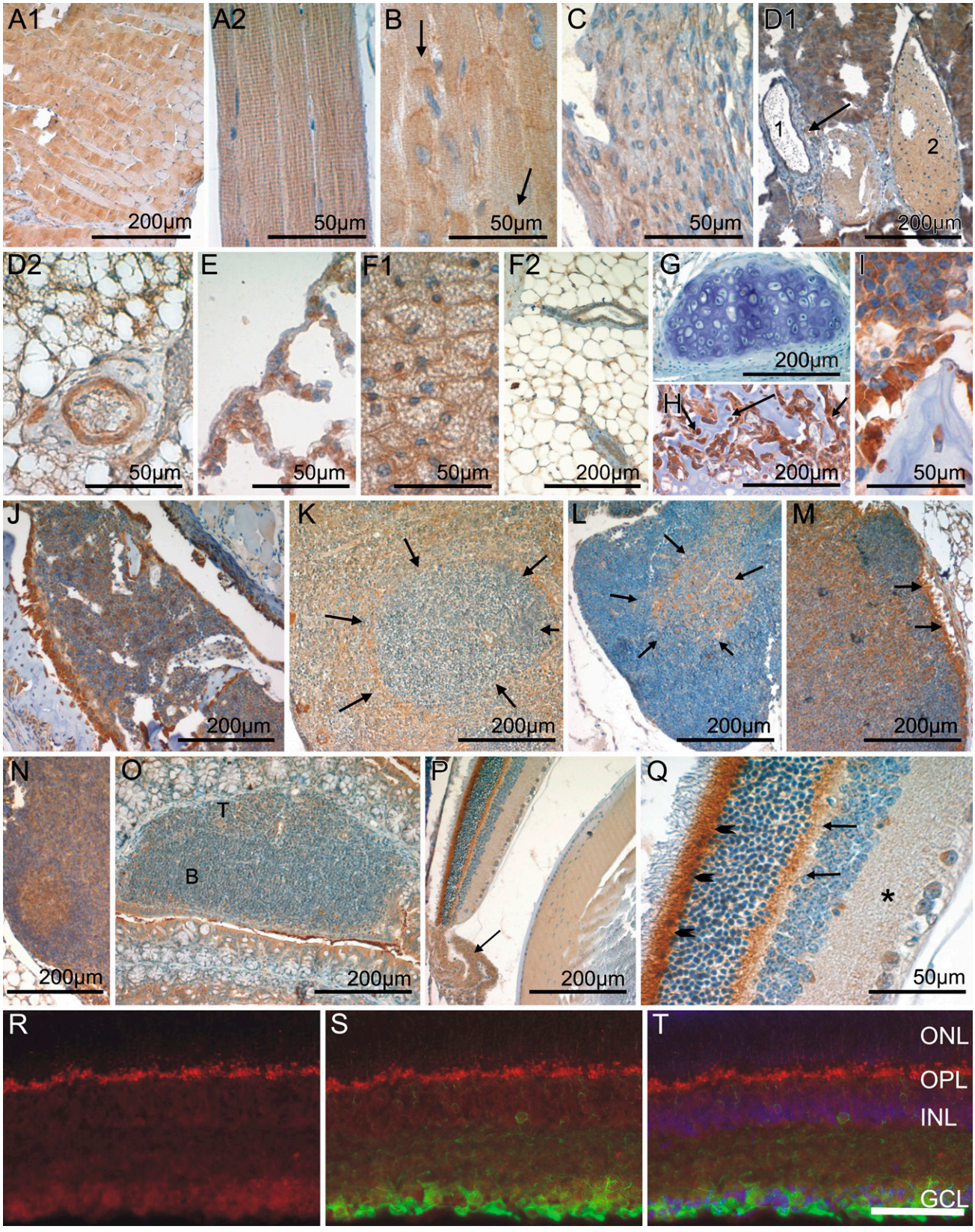

invasive carcinoma, T-Ag expression lingered in most tumors (Figure 5A), although in a small number of tumors, T-Ag was downregulated. CK1ε was detected in the cytoplasm of normal and neoplastic epithelial cells. In normal breast tissue of lactating mice, a strong CK1ε immunoreactivity was observed within the cytoplasm of ductal and acinar epithelial cells (Figure 5A). Upon neoplastic transformation to ductal carcinoma in situ (DCIS), CK1ε staining was downregulated. The lowest CK1ε immunoreactivity was observed in high-grade invasive carcinomas, i.e., those that are poorly differentiated (Figure 5A; Table 2). Correspondingly, on the RNA level, the expression of CK1ε was reduced in tumors of induced transgenic mice, compared with normal tissue of induced transgenic mice and non-transgenic mice (Figure 5B).

Discussion

CK1ε exhibits a variety of functions in eukaryotic cells. It is involved in the control of developmental processes, cell division, and circadian rhythm. Deregulation of CK1ε has been linked to pathophysiological processes such as carcinogenesis and neurodegeneration (Knippschild et al. 2005; Price 2006). However, amazingly little is known about the organ and cell type–specific distribution of CK1ε. To fill this gap and to obtain more information on its physiological role, we determined the expression of CK1ε in tissues and organs of young adult BALB/c mice. Furthermore, we assessed changes in the expression of CK1ε during tumorigenesis in a murine model of mammary carcinoma.

Western blot analysis revealed expression of CK1ε in all analyzed organs and tissues, with notably high protein levels in the brain and lung. Immunohistochemical staining using two different CK1ε-specific antibodies confirmed the ubiquitous expression patterns of CK1ε. We observed a distribution pattern for CK1ε similar to that recently described for CK1δ (Lohler et al. 2009). This may not be surprising in view of the high homology between CK1δ and CK1ε. A differential expression of CK1δ and CK1ε was observed in only a few cell types (summarized in Table 3). In the following, we will discuss our data on the background of previous findings describing cell type–specific functions of CK1ε.

Endocrine Tissue

CK1ε is highly expressed in endocrine organs, pointing to an involvement in the production, storage, and/or secretion of hormones, as previously described for other CK1 family members (Gross et al. 1997; Gross and Anderson 1998; Murakami et al. 1999; Behrend et al. 2000b; Knippschild et al. 2005; Lohler et al. 2009). We observed strong cytoplasmic CK1ε positivity in all three parts of the pituitary gland, indicating that CK1ε might be involved in specific functions of the SNARE complex and in neurotransmitter release, like CK1α and -δ (Gross et al. 1995; Shimazaki et al. 1996; Reisinger and Allerberger 1999; Kataoka et al. 2000; Pyle et al. 2000; Chheda et al. 2001; Dubois et al. 2002; Snyder et al. 2006; Wolff et al. 2006; Pozzi et al. 2008). In the testis, CK1ε positivity of Leydig cells suggests regulatory functions of CK1ε in vesicle transport and hormone release (Knippschild et al. 2005, and references therein). In the pancreas, CK1ε was weakly expressed in the exocrine part. In contrast, a high CK1ε immunoreactivity was observed in the Islets of Langerhans, with gradual differences in the expression level in individual islet cells. Similarly, gradual differences in CK1ε immunoreactivity were seen in cells of the adrenal and pituitary glands. Additional experiments are necessary to clarify whether CK1ε expression depends on the level of stimulation or the type of hormone-producing cell.

Immune System

Like CK1δ, CK1ε was found to be expressed in all lymphatic organs. Resting B lymphocytes in primary follicles and in the mantle zone of secondary follicles lacked CK1ε, whereas the germinal centers of secondary follicles, where activated B-cells predominate, expressed substantial levels of CK1ε. Thus, CK1ε positivity and activation status seemed to correlate in the B-cell compartment. Because several components of the

Figure 4 CK1ε expression in immobile cells of mesenchymal origin, in hematopoetic and lymphoid organs, and in the eye. Fixative: acid formalin, fixation by immersion. Peroxidase reaction, dye: DAB. CK1ε-specific antiserum 712 was used for immohistochemical staining of the following organs/tissues: skeletal muscle (**A1,A2**); myocardium (**B**); smooth muscle (**C**); arteriole, vein, and lymphatic vessel (**D1**); artery (**D2**); mesothelial cells of the pleura (**E**); brown (**F1**) and white (**F2**) fatty tissue; hyaline cartilage (**G**); osteoblasts and osteocytes (**H,I**); bone marrow (**J**); spleen (**K**); thymus (**L**); lymph node with primary (**M**) and secondary lymphoid follicle (**N**); cecal patch (**O**); eye (**P**); and retina (**Q**). In **B**, arrows indicate intercalated discs of cardiomyocytes. In **D1**, arrow indicates an arteriole, and numbers indicate a lymphatic vessel (1) and a vein (2). Arrows in **H** mark highly CK1ε-positive osteoblasts. In **K**, arrows outline a periarteriolar lymphoid sheath of the white pulp. Arrows in **L** delineate the medullary portion of the thymus. Arrows in **M** indicate strong CKIε-positive macrophages in the subcapsular sinus. In **O**, the B- and T-cell zones are marked with B and T, respectively. In **P**, arrow indicates the ciliary body. Arrowheads in **Q** indicate the inner segment of the photoreceptors, arrows point to the outer plexiform layer, and asterisk indicates the inner plexiform layer. Calibration bars in **A–Q** are as indicated. Immunohistochemical analysis of frozen retinal sections revealed localization of CK1ε in retinal ganglion cells (**R,T**, red), which were specifically costained with an anti-βIII-tubulin antibody (**S,T**, green) or DAPI (**T**, blue). ONL, outer nuclear layer; OPL, outer plexiform layer; INL, inner nuclear layer; GCL, retinal ganglion cell layer. Bar in **T** = 50 μm for **R–T**.

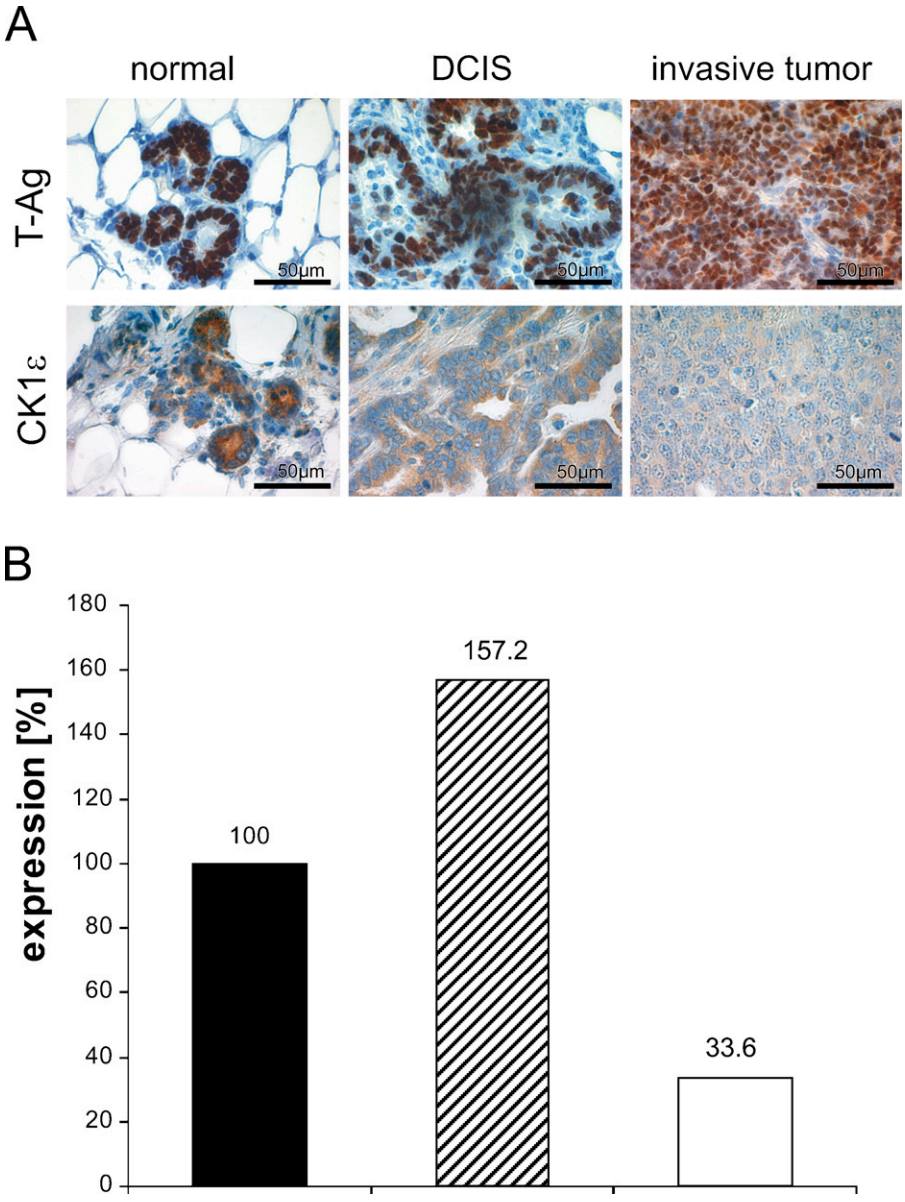

Figure 5 CK1ε expression in mammary epithelium is downregulated upon neoplastic transformation (**A**). For immunoperoxidase staining of CK1ε in normal mammary tissue (left), DCIS (middle), and invasive tumors (right) of WAP-T mice, CK1ε-specific antiserum 712 was used. Counterstaining with hemalaun was performed in all tissue sections. Immunostaining of T-Ag is shown in the top row, and CK1ε staining is shown in the bottom row. High CK1ε expression levels were detected in the cytoplasm of normal ductal and acinar epithelia cells (bottom left), whereas medium CK1ε levels were detected in ductal carcinoma in situ (bottom middle). The lowest expression was found in poorly differentiated tumors (bottom right). (**B**) Total RNA isolated from mammary tissue was reverse transcribed into cDNA. Expression of CK1ε was determined by real-time PCR. Relative CK1ε expression in breast carcinoma of induced WAP-T mice (black column) is compared with normal mammary tissue of induced WAP-T mice (gray column) and to mammary tissue of non-transgenic animals (white column).

B-cell activation process critically depend on nuclear factor 'kappa-light-chain-enhancer' of activated B-cells (NFκB), it is tempting to speculate that CK1ε might interfere with the regulation of the NFκB pathway in B lymphocytes. The CK1ε immunoreactivity seen in germinal centers might also indicate regulatory functions of CK1ε in proliferation, mobility, and antigen recognition. Our data are in line with previous reports showing an involvement of CK1δ/ε in lymphocyte physiology and a role of CK1ε in cytokine-induced differentiation of granulocytes (Maritzen et al. 2003; Okamura et al. 2004a). The adaptive immune system is remarkable for the high level of functional differentiation of its cellular components. No reliable morphological criteria are available to identify the multitude of immune cell types known today. Inasmuch as the data presented here provide a low-resolution image of the lymphoid system, it will be important to study CK1ε in immune cell subsets defined by a combination of their marker profile and microanatomical location. This could be achieved by using double immunofluorescence staining of lymphoid tissues or by examining CK1ε expression in distinct lymphoid tumor entities that represent the neoplastic counterpart of defined B-cell populations.

Central Nervous System

CK1ε expression in the brain revealed a widespread distribution similar to that described for CK1δ (Lohler et al. 2009), suggesting that the closely related CK1 isoforms exhibit similar biological functions. How-

Table 2 CK1ε expression in normal tissue, in situ carcinoma, and invasive tumors of SV40 T-Ag–induced transgenic mice

	CK1ε expression in		
Mouse	Normal tissue	In situ carcinoma	Invasive tumor
1	+++	++	+
2	+++	Ø	+
3	+++	Ø	+
4	+++	Ø	+
5	+++	Ø	+/++
6	+++	Ø	+
7	+++	Ø	+
8	+++	+	+/++
9	+++	+	+
10	+++	Ø	++
11	+++	Ø	+
12	++	+	+
13	+++	Ø	++
14	+++	+	+
15	+++	Ø	+
16	+++	Ø	+/++
17	+++	+	+
18	++	Ø	+

Intensity levels of CK1ε-specific staining were graded as: −, negative; +, weak; ++, moderate; or +++, strong. $^{+/++}$ Indicates weakly and moderately positive staining in tumor cells. Ø, no in situ carcinoma detected in the specimen.

ever, a few differences were detected (see also Table 3). In the cerebellum, Purkinje cells were strongly CK1δ positive, but negative for CK1ε. In contrast, astrocytes showed high CK1ε but no CK1δ immunoreactivity. The strong CK1ε positivity in neurons of various neuroanatomical compartments and the thalamus, and the heterogenous neuronal expression in the nuclei of the midbrain, pons, and medulla oblongata point to regulatory, cell type–specific functions of CK1ε in neuronal signal transduction and/or metabolism. These findings are in line with previous observations showing that CK1ε is involved in regulating the circadian rhythm and that deregulation of CK1 isoforms, especially those of CK1ε and -δ, lead to neurodegenerative disorders such as Alzheimer disease and circadian disorders (Greengard 2001; Takano et al. 2004; Chergui et al. 2005; Gould and Manji 2005; Meng et al. 2008; Bryant et al. 2009).

Reproductive Organs

In the testis, CK1ε expression was high in spermatogonia, i.e., the self-renewing pool of spermatogenesis characterized by a high mitotic rate. This indicates that CK1ε might be involved in the regulation of chromosome segregation and cell division, an assumption supported by several reports linking CK1 isoforms to mitosis and meiosis (Brockman et al. 1992; Horiguchi et al. 2005; Petronczki et al. 2006; Grozav et al. 2009). Upon maturation to spermatocytes, CK1ε was downmodulated to intermediate expression levels. Possibly, lower CK1ε amounts are engaged in meiotic cell division, compared with mitosis.

Table 3 Cell type–specific differences in the expression level of CK1δ and -ε

	CK1δ	CK1ε
Thymus		
Cortex thymocytes	$^{-/+}$	$^{-/++}$
Lymph node/MALT		
T zone	+	$^{++/-}$
Muscle cells		
Smooth	$^{+/-}$	++
Vascular endothelium		
High endothelial venoles	$^{+/-}$	++
Connective tissue		
Osteoblasts	−	+++
Osteocytes	−	+
Alimentary tract		
Esophageal squamous eptihelium (basal cell layer)	−	++
Stomach, parietal cells	−	++
Stomach, mucous neck cells	$^{+/+++}$	+
Intestine, globlet cells	−	$^{-/++}$
Intestine, paneth cells	−	$^{-/+}$
Urinary tract		
Collecting duct epithelium	$^{++/+++}$	+
Urothelium, umbrella cells	−	++
Female genital tract		
Oocytes	−	$^{+/++}$
Theka cells	−	+
Salivary glands		
Serous epithelial cells	$^{++/+++}$	−
Mucous epithelial cells	−	+
Pancreas		
Exocrine gland, acinar cells	++	$^{-/+}$
Liver		
Intrahepatic bile ducts	−	++
Eye		
Iris stroma	−	++
Retina		
Choroid	−	++
Inner nuclear layer	++	−
Ganglion cell layer	+++	+
Brain		
Purkinje cells/cerebellum	++	−
Astroglia	−	++

The expression patterns of CK1δ and -ε were compared in all tissues. Slash indicates simultaneous expression of different intensities, e.g., $^{-/++}$ indicates negative and moderately positive staining in one cell type. Cell types with considerable differences are listed.

Mammary Tumors of Induced SV40 T-Ag–transgenic Mice

We observed changes in the immunoreactivity of CK1ε in preinvasive and invasive breast carcinoma of SV40 T-Ag–transgenic mice. Whereas CK1ε is highly expressed in the cytoplasm of normal ductal and acinar cells, lower levels were detected in ductal carcinoma in situ. The lowest expression was found in poorly differentiated invasive tumors. The observed downregulation of CK1ε might be due to lack of differentiation of the mammary tumors. Alternatively, downregulation of CK1ε could provide a potential mechanism leading to the development of the chemoresistance of tumor cells,

especially to topoisomerase II drugs. The functions of topoisomerase IIα is regulated by site-specific phosphorylation, especially at Ser 1106 mediated by CK1δ and -ε. Hypophosphorylation of topoisomerase IIα at Ser 1106 correlates with resistance to topoisomerase II drugs and a reduced apoptosis rate (Grozav et al. 2009). Downregulation of CK1ε has also been described for human mammary cancer. Fuja et al. (2004) observed a correlation between immunohistological CK1ε staining intensity and tumor differentiation. However, considering the similarities of DCIS and invasive mammary carcinoma development in transgenic mice to the respective human diseases, it seems worthwhile to analyze in detail the prognostic relevance of changes in the expression of CK1ε and its highly homologous CK1δ in tumor development and progression.

In summary, the widespread distribution of CK1ε indicates its involvement in the regulation of various cellular processes. Our detailed anatomical profiling of CK1ε expression can be used in further studies to characterize cell type–specific functions of CK1ε and to determine pathophysiological alterations in various diseases. It will be particularly interesting to determine whether high CK1ε expression levels in cell populations with a negligible proliferative activity, such as some endocrine cells, hint of a yet-unknown function of this enzyme. The observed downregulation of CK1ε in mammary tumors of SV40 T-Ag–induced mice is similar to that in human tumors, and thus could be of clinical interest in the study of the development and progression of breast cancer. Further biochemical, molecular, and functional analyses in the transgenic mice model and in humans are needed to more precisely elucidate the significance of changes in the expression of CK1ε and to correlate CK1ε expression with clinical outcome.

Acknowledgments

This work was supported by Grant 108489 from the Deutsche Krebshilfe, Dr. Mildred Scheel Stiftung (to UK). The Heinrich-Pette-Institute is financially supported by the Freie und Hansestadt Hamburg and the Bundesministerium für Gesundheit.

We thank Dr. Jürgen Löhler for his advice and helpful discussions. We are grateful to Arnhild Grothey for her technical support.

Literature Cited

Amit S, Hatzubai A, Birman Y, Andersen JS, Ben-Shushan E, Mann M, Ben-Neriah Y, et al. (2002) Axin-mediated CKI phosphorylation of beta-catenin at Ser 45: a molecular switch for the Wnt pathway. Genes Dev 16:1066–1076

Bagheri-Yarmand R, Talukder AH, Wang RA, Vadlamudi RK, Kumar R (2004) Metastasis-associated protein 1 deregulation causes inappropriate mammary gland development and tumorigenesis. Development 131:3469–3479

Behrend L, Milne DM, Stoter M, Deppert W, Campbell LE, Meek DW, Knippschild U (2000a) IC261, a specific inhibitor of the protein kinases casein kinase 1-delta and -epsilon, triggers the mitotic checkpoint and induces p53-dependent postmitotic effects. Oncogene 19:5303–5313

Behrend L, Stoter M, Kurth M, Rutter G, Heukeshoven J, Deppert W, Knippschild U (2000b) Interaction of casein kinase 1 delta (CK1delta) with post-Golgi structures, microtubules and the spindle apparatus. Eur J Cell Biol 79:240–251

Beyaert R, Vanhaesebroeck B, Declercq W, Van Lint J, Vandenabele P, Agostinis P, Vandenheede JR, et al. (1995) Casein kinase-1 phosphorylates the p75 tumor necrosis factor receptor and negatively regulates tumor necrosis factor signaling for apoptosis. J Biol Chem 270:23293–23299

Brockman JL, Gross SD, Sussman MR, Anderson RA (1992) Cell cycle-dependent localization of casein kinase I to mitotic spindles. Proc Natl Acad Sci USA 89:9454–9458

Brockschmidt C, Hirner H, Huber N, Eismann T, Hillenbrand A, Giamas G, Radunsky B, et al. (2008) Anti-apoptotic and growth-stimulatory functions of CK1 delta and epsilon in ductal adenocarcinoma of the pancreas are inhibited by IC261 in vitro and in vivo. Gut 57:799–806

Bryant CD, Graham ME, Distler MG, Munoz MB, Li D, Vezina P, Sokoloff G, et al. (2009) A role for casein kinase 1 epsilon in the locomotor stimulant response to methamphetamine. Psychopharmacology (Berl) 203:703–711

Bustos VH, Marin O, Meggio F, Cesaro L, Allende CC, Allende JE, Pinna LA (2005) Generation of protein kinase Ck1alpha mutants which discriminate between canonical and non-canonical substrates. Biochem J 391:417–424

Camacho F, Cilio M, Guo Y, Virshup DM, Patel K, Khorkova O, Styren S, et al. (2001) Human casein kinase Idelta phosphorylation of human circadian clock proteins period 1 and 2. FEBS Lett 489:159–165

Chergui K, Svenningsson P, Greengard P (2005) Physiological role for casein kinase 1 in glutamatergic synaptic transmission. J Neurosci 25:6601–6609

Chheda MG, Ashery U, Thakur P, Rettig J, Sheng ZH (2001) Phosphorylation of Snapin by PKA modulates its interaction with the SNARE complex. Nat Cell Biol 3:331–338

Davidson G, Wu W, Shen J, Bilic J, Fenger U, Stannek P, Glinka A, et al. (2005) Casein kinase 1 gamma couples Wnt receptor activation to cytoplasmic signal transduction. Nature 438:867–872

Deppert W, Pates R (1979) Cell surface location of simian virus 40-specific proteins on HeLa cells infected with adenovirus type 2-simian virus 40 hybrid viruses Ad2+ND1 and Ad2+ND2. J Virol 31:522–536

Desagher S, Osen-Sand A, Montessuit S, Magnenat E, Vilbois F, Hochmann A, Journot L, et al. (2001) Phosphorylation of bid by casein kinases I and II regulates its cleavage by caspase 8. Mol Cell 8:601–611

Dubois T, Kerai P, Learmonth M, Cronshaw A, Aitken A (2002) Identification of syntaxin-1A sites of phosphorylation by casein kinase I and casein kinase II. Eur J Biochem 269:909–914

Ebisawa T, Uchiyama M, Kajimura N, Mishima K, Kamei Y, Katoh M, Watanabe T, et al. (2001) Association of structural polymorphisms in the human period3 gene with delayed sleep phase syndrome. EMBO Rep 2:342–346

Elias L, Li AP, Longmire J (1981) Cyclic adenosine 3′:5′-monophosphate-dependent and -independent protein kinase in acute myeloblastic leukemia. Cancer Res 41:2182–2188

Frierson HF Jr, El-Naggar AK, Welsh JB, Sapinoso LM, Su AI, Cheng J, Saku T, et al. (2002) Large scale molecular analysis identifies genes with altered expression in salivary adenoid cystic carcinoma. Am J Pathol 161:1315–1323

Fuja TJ, Lin F, Osann KE, Bryant PJ (2004) Somatic mutations and altered expression of the candidate tumor suppressors CSNK1 epsilon, DLG1, and EDD/hHYD in mammary ductal carcinoma. Cancer Res 64:942–951

Gould TD, Manji HK (2005) DARPP-32: a molecular switch at the nexus of reward pathway plasticity. Proc Natl Acad Sci USA 102:253–254

Greengard P (2001) The neurobiology of dopamine signaling. Biosci Rep 21:247–269

Gross SD, Anderson RA (1998) Casein kinase I: spatial organization and positioning of a multifunctional protein kinase family. Cell Signal 10:699–711

Gross SD, Hoffman DP, Fisette PL, Baas P, Anderson RA (1995) A phosphatidylinositol 4,5-bisphosphate-sensitive casein kinase I alpha associates with synaptic vesicles and phosphorylates a subset of vesicle proteins. J Cell Biol 130:711–724

Gross SD, Simerly C, Schatten G, Anderson RA (1997) A casein kinase I isoform is required for proper cell cycle progression in the fertilized mouse oocyte. J Cell Sci 110:3083–3090

Grozav AG, Chikamori K, Kozuki T, Grabowski DR, Bukowski RM, Willard B, Kinter M, et al. (2009) Casein kinase I delta/epsilon phosphorylates topoisomerase IIalpha at serine-1106 and modulates DNA cleavage activity. Nucleic Acids Res 37:382–392

Horiguchi R, Tokumoto M, Nagahama Y, Tokumoto T (2005) Molecular cloning and expression of cDNA coding for four spliced isoforms of casein kinase Ialpha in goldfish oocytes. Biochim Biophys Acta 1727:75–80

Izeradjene K, Douglas L, Delaney A, Houghton JA (2004) Influence of casein kinase II in tumor necrosis factor-related apoptosis-inducing ligand-induced apoptosis in human rhabdomyosarcoma cells. Clin Cancer Res 10:6650–6660

Kataoka M, Kuwahara R, Iwasaki S, Shoji-Kasai Y, Takahashi M (2000) Nerve growth factor-induced phosphorylation of SNAP-25 in PC12 cells: a possible involvement in the regulation of SNAP-25 localization. J Neurochem 74:2058–2066

Knippschild U, Gocht A, Wolff S, Huber N, Lohler J, Stoter M (2005) The casein kinase 1 family: participation in multiple cellular processes in eukaryotes. Cell Signal 17:675–689

Kuret J, Johnson GS, Cha D, Christenson ER, DeMaggio AJ, Hoekstra MF (1997) Casein kinase 1 is tightly associated with paired-helical filaments isolated from Alzheimer's disease brain. J Neurochem 69:2506–2515

Liu C, Li Y, Semenov M, Han C, Baeg GH, Tan Y, Zhang Z, et al. (2002) Control of beta-catenin phosphorylation/degradation by a dual-kinase mechanism. Cell 108:837–847

Lohler J, Hirner H, Schmidt B, Kramer K, Fischer D, Thal DR, Leithauser F, et al. (2009) Immunohistochemical characterisation of cell-type specific expression of CK1delta in various tissues of young adult BALB/c mice. PLoS One 4:e4174

Marin O, Bustos VH, Cesaro L, Meggio F, Pagano MA, Antonelli M, Allende CC, et al. (2003) A noncanonical sequence phosphorylated by casein kinase 1 in beta-catenin may play a role in casein kinase 1 targeting of important signaling proteins. Proc Natl Acad Sci USA 100:10193–10200

Maritzen T, Lohler J, Deppert W, Knippschild U (2003) Casein kinase I delta (CKIdelta) is involved in lymphocyte physiology. Eur J Cell Biol 82:369–378

Meng QJ, Logunova L, Maywood ES, Gallego M, Lebiecki J, Brown TM, Sladek M, et al. (2008) Setting clock speed in mammals: the CK1 epsilon tau mutation in mice accelerates circadian pacemakers by selectively destabilizing PERIOD proteins. Neuron 58:78–88

Milne DM, Looby P, Meek DW (2001) Catalytic activity of protein kinase CK1 delta (casein kinase 1delta) is essential for its normal subcellular localization. Exp Cell Res 263:43–54

Murakami A, Kimura K, Nakano A (1999) The inactive form of a yeast casein kinase I suppresses the secretory defect of the sec12 mutant. Implication of negative regulation by the Hrr25 kinase in the vesicle budding from the endoplasmic reticulum. J Biol Chem 274:3804–3810

Okamura A, Iwata N, Nagata A, Tamekane A, Shimoyama M, Gomyo H, Yakushijin K, et al. (2004a) Involvement of casein kinase Iepsilon in cytokine-induced granulocytic differentiation. Blood 103:2997–3004

Okamura H, Garcia-Rodriguez C, Martinson H, Qin J, Virshup DM, Rao A (2004b) A conserved docking motif for CK1 binding controls the nuclear localization of NFAT1. Mol Cell Biol 24:4184–4195

Peters JM, McKay RM, McKay JP, Graff JM (1999) Casein kinase I transduces Wnt signals. Nature 401:345–350

Petronczki M, Matos J, Mori S, Gregan J, Bogdanova A, Schwickart M, Mechtler K, et al. (2006) Monopolar attachment of sister kinetochores at meiosis I requires casein kinase 1. Cell 126:1049–1064

Pozzi D, Condliffe S, Bozzi Y, Chikhladze M, Grumelli C, Proux-Gillardeaux V, Takahashi M, et al. (2008) Activity-dependent phosphorylation of Ser187 is required for SNAP-25-negative modulation of neuronal voltage-gated calcium channels. Proc Natl Acad Sci USA 105:323–328

Price MA (2006) CKI, there's more than one: casein kinase I family members in Wnt and Hedgehog signaling. Genes Dev 20:399–410

Pyle RA, Schivell AE, Hidaka H, Bajjalieh SM (2000) Phosphorylation of synaptic vesicle protein 2 modulates binding to synaptotagmin. J Biol Chem 275:17195–17200

Reisinger EC, Allerberger F (1999) Bacterial resistance, beta-lactam antibiotics and gramnegative bacteria at ICUs. Wien Klin Wochenschr 111:537–538

Schulze-Garg C, Lohler J, Gocht A, Deppert W (2000) A transgenic mouse model for the ductal carcinoma in situ (DCIS) of the mammary gland. Oncogene 19:1028–1037

Schwab C, DeMaggio AJ, Ghoshal N, Binder LI, Kuret J, McGeer PL (2000) Casein kinase 1 delta is associated with pathological accumulation of tau in several neurodegenerative diseases. Neurobiol Aging 21:503–510

Shimazaki Y, Nishiki T, Omori A, Sekiguchi M, Kamata Y, Kozaki S, Takahashi M (1996) Phosphorylation of 25-kDa synaptosome-associated protein. Possible involvement in protein kinase C-mediated regulation of neurotransmitter release. J Biol Chem 271:14548–14553

Snyder DA, Kelly ML, Woodbury DJ (2006) SNARE complex regulation by phosphorylation. Cell Biochem Biophys 45:111–123

Stoter M, Bamberger AM, Aslan B, Kurth M, Speidel D, Loning T, Frank HG, et al. (2005) Inhibition of casein kinase I delta alters mitotic spindle formation and induces apoptosis in trophoblast cells. Oncogene 24:7964–7975

Swiatek W, Kang H, Garcia BA, Shabanowitz J, Coombs GS, Hunt DF, Virshup DM (2006) Negative regulation of LRP6 function by casein kinase I epsilon phosphorylation. J Biol Chem 281:12233–12241

Takano A, Hoe HS, Isojima Y, Nagai K (2004) Analysis of the expression, localization and activity of rat casein kinase 1epsilon-3. Neuroreport 15:1461–1464

Takenaka Y, Fukumori T, Yoshii T, Oka N, Inohara H, Kim HR, Bresalier RS, et al. (2004) Nuclear export of phosphorylated galectin-3 regulates its antiapoptotic activity in response to chemotherapeutic drugs. Mol Cell Biol 24:4395–4406

Toh KL, Jones CR, He Y, Eide EJ, Hinz WA, Virshup DM, Ptacek LJ, et al. (2001) An hPer2 phosphorylation site mutation in familial advanced sleep phase syndrome. Science 291:1040–1043

Walter J, Grunberg J, Schindzielorz A, Haass C (1998) Proteolytic fragments of the Alzheimer's disease associated presenilins-1 and -2 are phosphorylated in vivo by distinct cellular mechanisms. Biochemistry 37:5961–5967

Wolff S, Stoter M, Giamas G, Piesche M, Henne-Bruns D, Banting G, Knippschild U (2006) Casein kinase 1 delta (CK1delta) interacts with the SNARE associated protein snapin. FEBS Lett 580:6477–6484

Xu Y, Padiath QS, Shapiro RE, Jones CR, Wu SC, Saigoh N, Saigoh K, et al. (2005) Functional consequences of a CKIdelta mutation causing familial advanced sleep phase syndrome. Nature 434:640–644

Yasojima K, Kuret J, DeMaggio AJ, McGeer E, McGeer PL (2000) Casein kinase 1 delta mRNA is upregulated in Alzheimer disease brain. Brain Res 865:116–120

Zeng X, Tamai K, Doble B, Li S, Huang H, Habas R, Okamura H, et al. (2005) A dual-kinase mechanism for Wnt co-receptor phosphorylation and activation. Nature 438:873–877

Zhao Y, Qin S, Atangan LI, Molina Y, Okawa Y, Arpawong HT, Ghosn C, et al. (2004) Casein kinase 1alpha interacts with retinoid X receptor and interferes with agonist-induced apoptosis. J Biol Chem 279:30844–30849

The Journal of Histochemistry & Cytochemistry